Detecting Rat's Kidney Inflammation Using Real Time Photoacoustic Tomography

M. Y. Lee, D. H. Shin, S. H. Park, W.C. Ham, S.K. Ko, C. G. Song

Abstract—Photoacoustic Tomography (PAT) is a promising medical imaging modality that combines optical imaging contrast with the spatial resolution of ultrasound imaging. It can also distinguish the changes in biological features. But, real-time PAT system should be confirmed due to photoacoustic effect for tissue. Thus, we have developed a real-time PAT system using a custom-developed data acquisition board and ultrasound linear probe. To evaluate performance of our system, phantom test was performed. As a result of those experiments, the system showed satisfactory performance and its usefulness has been confirmed. We monitored the degradation of inflammation which induced on the rat's kidney using real-time PAT.

Keywords—Photoacoustic tomography, inflammation detection, rat, kidney, contrast agent, ultrasound.

I. Introduction

PAT, referred to optoacoustic tomography or thermoacoustic tomography, is an emerging hybrid imaging modality which is noninvasive, nonionizing. It has also satisfactory imaging depth, good temporal resolution, good spatial resolution and high sensitivity [1]-[5].

PAT images detect targets that absorb electromagnetic waves. If a short-pulsed laser source is irradiated onto an object, some of the energy is absorbed and converted into heat. The heating causes thermoelastic expansion, which temporarily produces broadband acoustic waves. This type of acoustic pressure is called a photoacoustic wave and can be measured by ultrasonic transducers at various locations around object surface for image reconstruction [6]-[8].

PAT imaging is a hybrid imaging modality which combines optical contrast and ultrasound resolution. Pure optical imaging has great contrast, but it cannot image tissue that is in deep. But photoacoustic imaging (PAI) can acquire the high imaging contrast and overcomes some weaknesses of optical imaging by using acoustic measurements. In addition, because of different optical absorption coefficient between biological components of tissue, PAI can detect the signal due to photoacoustic effect. Thus, PAI technique is mainly adapted to skin disease, rheumatoid arthritis, breast cancer and prostate cancer diagnosis applications [16]-[18].

M. Y Lee, D.H. Shin, S.H. Park, S.K. Ko, and C. G Song are with the Department of Electronics Engineering, Center for Advanced Image and Information Technology of Chonbuk National University, South Korea (phone: 82-10-9449-6206, 82-10-5534-0257, 82-10-2016-8984, 82-10-5038-8342, 82-10-2541-8531, respectively; e-mail: lmy6206@gmail.com, skear@naver.com, magellna0608@naver.com, gosk6363@navel.com, song133436@gmail.com, respectively).

W.C. Ham is with the Department of Electronics Engineering, of Chonbuk National University, South Korea (phone: 82-270-2405; e-mail: wcham@jbnu.ac.kr).

Recently, researches are underway on real-time PAT techniques to acquire images of bio tissue functions in more non-invasive targets. Real-time photoacoustic image devices are developed using an array transducer embedded with multiple ultrasound transducers. In order to overcome limit of the linear array transducer and visualize the target in 3D, 2D array transducer-based imaging acquisition PAI system was announced [11], [12].

PAI could be exposed to noises due to many different reasons. Noise can be generated due to not only the imaging device's internal noise or the low sensitivity to ultrasound signal and size of a detector but also the size assumed by an image reconstruction algorithm. These noises prevent the interpretation of the acquired images, thus we could not diagnose the disease well. So noise elimination is essential for the process [13]-[15].

To confirm the reaction due to photoacoustic effect using PAI method *in vivo*, real-time PAT systems have recently been studied in many research groups. In other studies, linear array probes for ultrasound imaging, in which a large number of transducers are linearly embedded, have been used as real-time PAT systems, but only for experiments with small animals [19]-[21].

Since the systems have a limited angular view, this causes distortion and reduces the resolution in the obtained images [8]-[10].

The purpose of this research is to evaluate the utility of PAT system. We conducted an experiment to detect the position of inflammation using real-time PAT and ultrasound system by injecting contrast agent into kidney.

II. Material and Methods

A. Proposed PAT System

Photoacoustic system measures photoacoustic data in real-time with ultrasound transducer. Also, pulsed laser source, acquisition of signal and reconstruction of imaging must be made successively. In order to meet these conditions, PXI platform based DAQ board was used. The PXI platform is equipped with 128 analog input channels, 50 MHz sampling frequency and 12 bit resolution power. Also, it can communicate to PC with the 192 Mb/s through direct memory access (DMA).

We used the laser trigger to synchronize between light emission and acquisition of data. We also used a linear array probe (L14-5/38, Ultrasonix) to detect the signal with 128 elements that have central frequency of 5 MHz.

In order to amplify signal and reduce the noise, we made the pre-amplifier with 128 channel, 40 dB gain, and 7.5 MHz

bandwidth and pre-amplifier was disposed at the front side of DAQ board. Acquired image has 488 × 400 pixels with resolution of 0.08 mm × 0.08 mm for each pixel.

Fig. 1 shows the schematic of the real-time PAT image acquisition system.
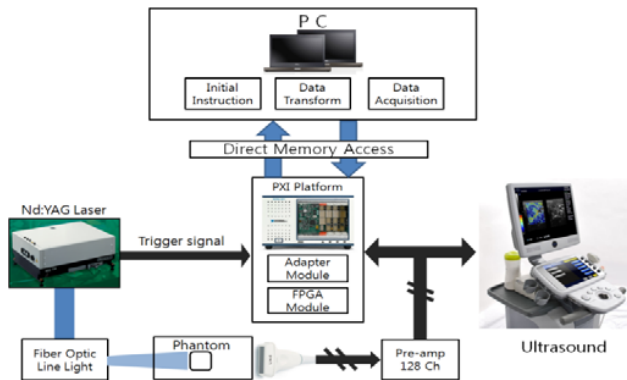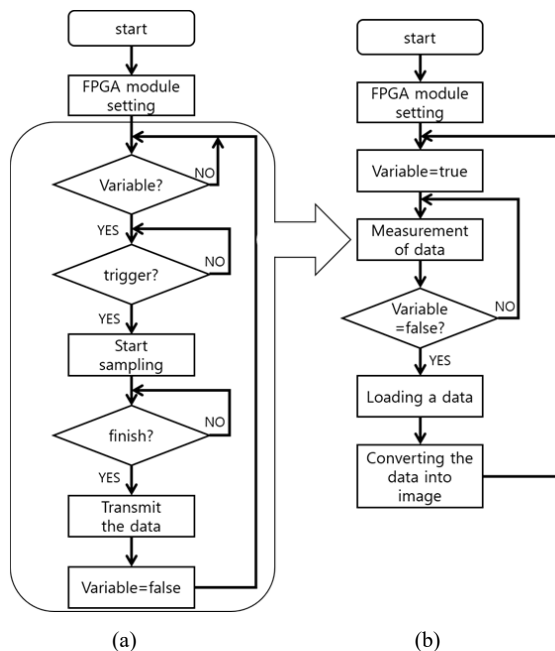

Fig. 1 Schematic of real-time PAT hardware

Fig. 2 Program flow chart (a) FPGA (b) Host

B. FPGA Program

A real-time PAT program is composed to two different platforms. First, PXI platform runs to control the FPGA program. The function of FPGA program is used to measure the signal with 50 MHz sampling frequency and transmit the signal into PC. Second, PC (host program) is used to reconstruct the image using received PA signal to FPGA. The host program also controls the FPGA program, reconstruction of image and synchronization for entire system we use. The PAT system depends on the host program because the FPGA is faster than PC.

Fig. 2 depicts a flow chart of the entire PAT acquisition. To synchronize each program, one flag bit is used to indicate the present process. Each program can read or change the flag to determine the next step.

If the host program is ready to measure, it changes a flag bit to false, and the FPGA program progresses its sequence. After detecting a trigger signal, 2500 data sets of PA signals from the array probe are sampled and stored in the DMA buffer, and flag bit is changed again. Finally, the host program reads the data from the PXI to the PC and reconstructs the image.

C. Back Projection Algorithm

The universal back projection algorithm [8] is used to reconstruct the PA images. The property of this algorithm is time domain PAT reconstruction.

The advantage of the back projection algorithm is that this uses the inverse property of the photoacoustic equations. The back projection algorithm offers an accurate solution along three fundamental geometries for reconstruction.

The Fourier domain formulas for reconstruction are the basic geometries that are simplified to a universal back projection formula.

$$P_0 = \int_{\Omega_0} \frac{d\Omega_0}{\Omega_0}\left[2p(\overrightarrow{r_0}, v_s t) - 2v_s t \frac{\partial p(\overrightarrow{r_0}, v_s t)}{\partial(v_s t)}\right] \tag{1}$$

where, $\overrightarrow{r_0}$ is the measurement point, and v_s is the speed of sound. The t is given by,

$$t = \left|\vec{r} - \frac{\overrightarrow{r_0}}{v_s}\right|$$

The vectors of the image plane that required to be calculated are given as $\vec{r}$. The initial distribution of the photoacoustic pressure and the final measured photoacoustic signal is given by P_0 and $p(\overrightarrow{r_0}, v_s t)$, respectively. The exact time domain and results can be obtained by assuming a constant speed of sound. This algorithm uses the property of limited angular method to acquire the signal, which is able to use the linear array transducers.

When we use many elements for transducer, the system can reconstruct accurate photoacoustic images. The use of the solid angle can improve the variations of the single transducer views. It can be modified or extended to some forms of source inverse diffraction tomographic techniques. If the algorithm is acoustically inhomogeneous, it can result in the distortions.

III. EXPERIMENT

To evaluate the feasibility and performance of our PAT system, we took the two different experiments.

First, we measured the resolution. The gelatin with rectangular shape (protein: 84 ~ 90%, water: 8 ~ 12%) is prepared to mimic the biological tissue, and embedded cross pattern of hair with 0.03 mm diameter.

The source was an Nd: YAG laser (NT352-A20-AW, EKSPLA) with 680 nm wavelength, and the repetition rate was 2 Hz. Because the measurement area is much bigger than the beam profile, Fiber Optic Line Light (NT57-019, Edmund Optics) was used for expansion. The linear array probe and

Fiber Optic Line Light were fixed on the optical table to prevent motion artifacts.

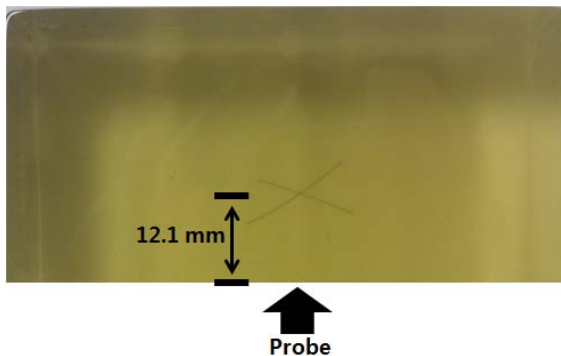Fig. 3 is the mimicking biological tissue phantom that embed the cross pattern of hair.

Fig. 3 Phantom of Hair

A. Resolution Phantom Experiment

The result of this experiment is shown in Fig. 4. Fig. 4 shows thickness that is 10 times thicker than the 0.03 mm hair thickness. Since we assume that the acoustic speed is 1500 m/sec and the transducer has a 5 MHz center frequency, the resolution of system we predict is approximately 0.15 mm, which is not enough to detect the actual hair thickness. Thus, the result of this experiment is predicted to show the maximum resolution of our PAT system, which was approximately 0.3 mm.

Through the first Phantom experiment, we verified the resolution of PAT system.
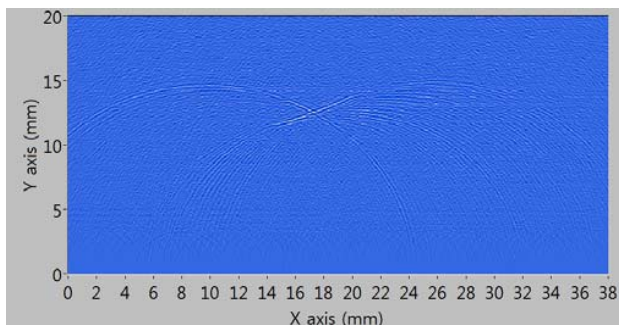

Fig. 4 Reconstruction image with Fig. 3

B. Animal Experiment

In second experiment, we use the PAT system in animal experiment. We use the contrast agent called Indo-cyanine green. This contrast agent has the best reactivity when the laser is irradiated at 800 nm.

For animal experiment, we use 8-weeks old SD rat. There are two types of SD rat we use. First is inflammation-induced and second is the normal rat for control.

In order to anesthetize the rat, we mixed the zoletile, rompum, and saline solution with 1:2.5:9. After anesthetizing the rat, we injected indo-cyanine green and histamine into kidney. Histamine is used to conduct the therapy for inflammation.

Finally, we measured the kidney to ultrasound device, then PA image.

In Fig. 5 (a) we took the image for inflammation-induced kidney, and we could detect the inflammation area in PAT system (refer to the circled point). But in case of control kidney, we could not detect any signal. Consequently, we could verify the inflammation area compare with normal kidney.
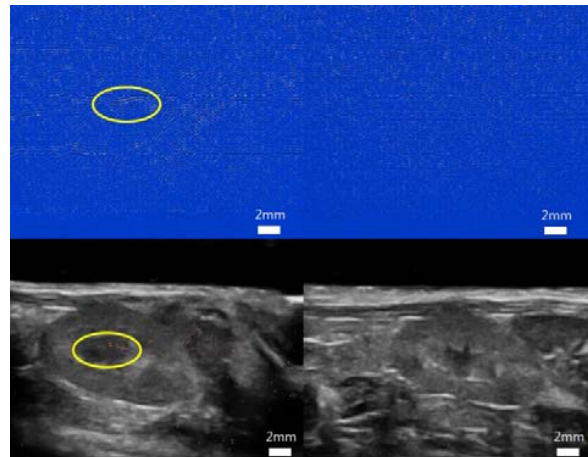

Fig. 5 Overlaid image with PAT and ultrasound obtained by injecting Contrast agent & Histamine into Kidney

IV. CONCLUSION

In this study, we developed the real-time PAT system for diagnosis and confirm the performance through phantom test for resolution.

Phantom test shows that our system could be enough to obtain a 570 * 300 pixel image at 2 frames/sec and 0.15 mm. Real-time PAT system depended on the laser radiation speed in order to synchronize between radiation and detection. Maximum laser source repetition rate was 10 Hz, and the system showed the 5 frame/ sec. But the SNR of image is poor because laser's repetition reduces the power of that.

In animal experiment, it is possible to detect the inflammation with our system using Indo-cyanine green. However, because Indo-cyanine green is not completely focused to the inflamed area, acquired signal is very weak. In order to overcome this problem, we need the special contrast agent that could target the inflammation.

REFERENCES

[1] Oraevsky A A, Jacques S L, Esenaliev R O, Tittel F K, Time-resolved optoacoustic imaging in layered biological tissues, Advances in Optical Imaging and Photon Migrationed R R Alfano (New York: Academic) pp 161.5, 1994
[2] Kruger R A, Photo-acoustic ultrasound: pulse production and detection in 0.5% Liposyn, Med. Phys. 21 127.31, 1994
[3] Kruger R A, Liu P-Y, Fang Y, Thermoacoustic ultrasound (PAUS)-reconstruction tomography, Med. Phys.22 1605.9, 1995
[4] Oraevsky A A, Esenaliev R O, Jacques S L, Tittel S K, Laser

opto-acoustic tomography for medical diagnostics: principles, Proc. SPIE 2976 22.31, 1996

[5] Hoelen C G A, de Mul F F M, Pongers R, Dekker A, Three-dimensional photoacoustic imaging of blood vessels in tissue, Opt. Lett. 23 648-650, 1998

[6] A. Oraevsky and A. Karabutov, Optoacoustic tomography, in Biomedical Photonics Handbook, T. Vo-Dinh, CRC, Boca Raton, Ed., Chap. 34, pp. 1-34, 2003.

[7] L. V. Wang and H. Wu, Ed. Biomedical Optics: Principles and Imaging, John Wiley, 2007.

[8] Lihong V. Wang, Ed. Photoacoustic Imaging and Spectroscopy, 1st ed., Boca Raton: CRC Press, 2009.

[9] J. T. Oh, M. L. Li, H. F. Zhang, K. Maslov, G. Stoica, and L. V. Wang, Three-dimensional imaging of skin melaNoma in vivo by dual-wavelength photoacoustic microscopy, J. Biomed. Opt., Vol. 11, No. 3, p. 034032, Nov. 2006.

[10] S. Yang, D. Xing, Q. Zhou, L. Xiang, and Y. Lao, Functional imaging of cerebrovascular activities in small animals using high-resolution photoacoustic tomography, Med. Phys., Vol. 34, No. 8, p. 3294-3301, Aug. 2007

[11] Q. Zhou, X. Ji and D. Xing, Full-field 3D photoacoustic imaging based on plane transducer array and spatial phase-controlled algorithm, Med. Phys. 38(3), 1561 (2011).

[12] J. Gamelin, A. Maurudis, A. Aguirre, F. Huang, P. Guo, L. V. Wang and Q. Zhu, A real-time photoacoustic tomography system for small animals, Optics Express 10489, 17(13), 22 (2009).

[13] V. Moock, C. Garcia-Segundo, E. Garduno, F. Arambula Cosio, J. Jithin, P. van Es, S. Manohar and W. Steenbergen, Signal Processing for Photoacoustic Tomography, IEEE CISP 2012, 957 (2012).

[14] Y. Zhang, Y. Wang, An Improved Filtered Back-Projection Algorithm for Photoacoustic Tomography, IEEE iCBBE 2011, 1 (2011).

[15] T. Oruganti, J. G. Laufer and B. E. Treeby, Vessel filtering of photoacoustic images, Proc. SPIE 8581, 85811W (2013).

[16] J. T. Oh, M. L. Li, H. F. Zhang, K. Maslov, G. Stoica and L. V. Wang, Three-dimensional imaging of skin melanoma in vivo by dual-wavelength photoacoustic microscopy, J. Biomed. Opt. 11(3), 34032 (2006).

[17] S. Manohar, A. Kharine, J. C. van Hespen, W. Steenbergen and T. G. van Leeuwen, The twente photoacoustic mammoscope: system overview and performance, Phys. Med. Biol. 50(11), 2543 (2005).

[18] S. A. Ermilov, R. Gharieb, A. Conjusteau and A. A. Oraevsky, Hybrid optoacoustic and ultrasonic imaging system for detection of prostate malignancies, Proc. SPIE 6856, 68560T (2008).

[19] J. T. Oh, M. L. Li, H. F. Zhang, K. Maslov, G. Stoica, and L. V. Wang, Three-dimensional imaging of skin melaNoma in vivo by dual-wavelength photoacoustic microscopy, J. Biomed. Opt., Vol. 11, No. 3, p. 034032, Nov. 2006.

[20] S. Yang, D. Xing, Q. Zhou, L. Xiang, and Y. Lao, Functional imaging of cerebrovascular activities in small animals using high-resolution photoacoustic tomography, Med. Phys., Vol. 34, No. 8, p. 3294-3301, Aug. 2007

[21] E. Z. Zhang, J. G. Laufer, R. B. Pedley, and P. C. Beard, In vivo high-resolution 3D photoacoustic imaging of superficial vascular anatomy, Phys. Med. Biol., Vol. 54, No. 4, p. 1035-1046, Jan. 2009